

promoting access to White Rose research papers



Universities of Leeds, Sheffield and York
<http://eprints.whiterose.ac.uk/>

This is an author produced version of a paper published in **Industrial and Engineering Chemistry Research**.

White Rose Research Online URL for this paper:
<http://eprints.whiterose.ac.uk/3648/>

Published paper

Nimmo.W., Patsias A.A. & Hall, W. J (2005) *Characterization of a process for the in-furnace reduction of NO_x, SO₂, and HCl by carboxylic salts of calcium*, Industrial and Engineering Chemistry Research, Volume 44 (12), 4484 - 4494.

Characterization of a Process for the In-Furnace Reduction of NO_x, SO₂, and HCl by Carboxylic Salts of Calcium

W. Nimmo, A. A. Patsias, W. J. Hall, and P. T. Williams*

ABSTRACT

Calcium magnesium acetate has been assessed as an agent for the reduction of NO_x, SO₂, and HCl, at the pilot scale, in a down-fired combustor operating at 80 kW_{th}. In addition to this, the chemical and physical processes that occur during heating have been investigated. Benchmarking of calcium magnesium acetate with a suite of five other carboxylic salts (calcium magnesium acetate, calcium propionate, calcium acetate, calcium benzoate, magnesium acetate, and calcium formate) has been performed. NO_x reduction involves the volatile organic content of the carboxylic salt being released at temperatures of >1000 °C, where the reaction of CH_i radicals with NO under fuel-rich conditions can result in some of the NO forming N₂ in a “reburning” process. Thermogravimetry-Fourier transform infrared (TG-FTIR) studies identified the nature of the decomposition products from the low- and high-temperature decompositions. In addition, the rate of weight losses were studied to investigate the influence of the organic decomposition on NO_x reduction by reburning. In-furnace reductions of SO₂ and HCl are aided by the highly porous, particulate residue, which results from the in situ drying, pyrolysis, and calcination processes. Simultaneous reduction of all three pollutants was obtained, and a synergy between SO₂ and HCl capture was identified. A mechanism for this inter-relationship has been proposed. Sorbent particle characterization has been performed by collecting the calcined powder from a spray pyrolysis reactor and compared with those produced from a suite of pure carboxylic salts. Physical properties (including porosity, surface area, and decomposition behavior) have been discussed, relative to reductions in NO_x and acid gas emissions.

TABLES AND FIGURES

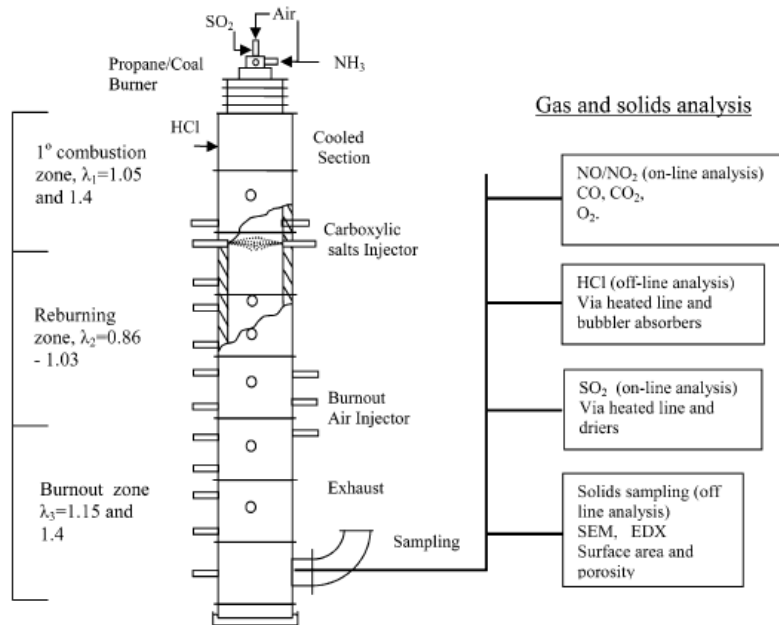


Figure 1. Schematic diagram of the 80-kW down-fired furnace, showing primary, reburn, and burn-out combustion zones.

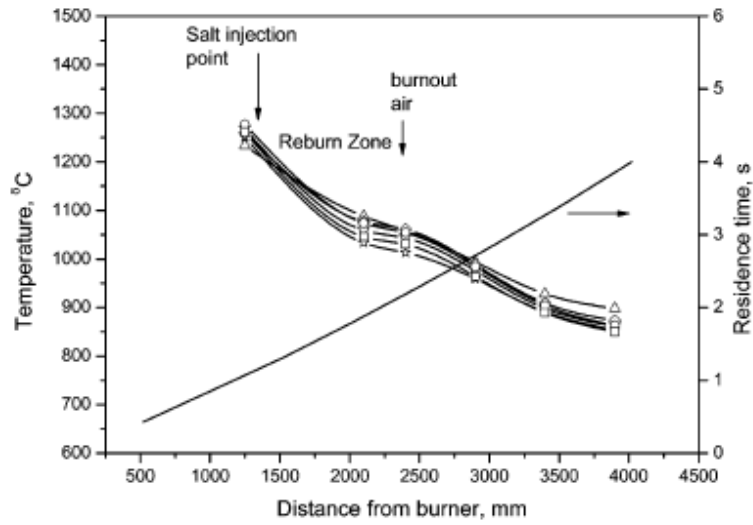


Figure 2. Temperature profiles and residence times for the 80-kW furnace: (Δ) calcium magnesium acetate (CMA), (∇) calcium propionate (CP), ($*$) calcium benzoate (CB), (\diamond) calcium acetate (CA), (\bullet) magnesium acetate (MA), and (\square) calcium formate (CF).

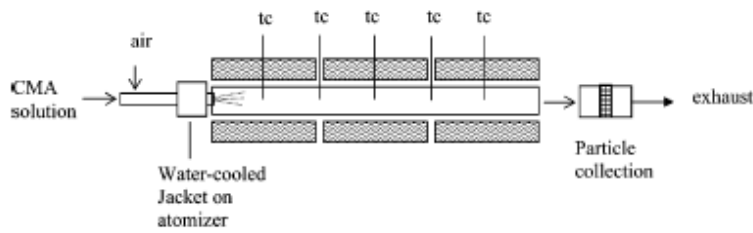


Figure 3. Schematic diagram of the calcination reactor.

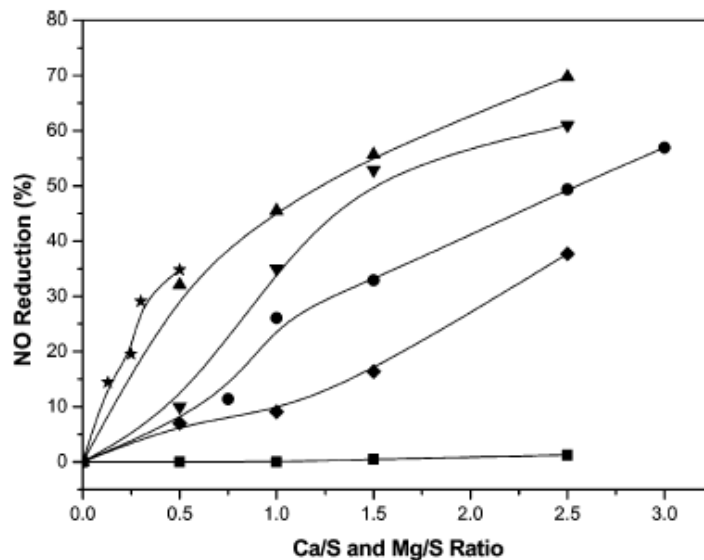


Figure 4. Effect of feed rate on NO reduction for (\blacktriangle) CMA, (\blacktriangledown) CP, (\blackstar) CB, (\blacklozenge) CA, (\bullet) MA, and (\blacksquare) CF, under reburning conditions of $\lambda_1 = 1.05$, $\lambda_2 = 1.03-0.86$, and $\lambda_3 = 1.15$ (3% O_2).

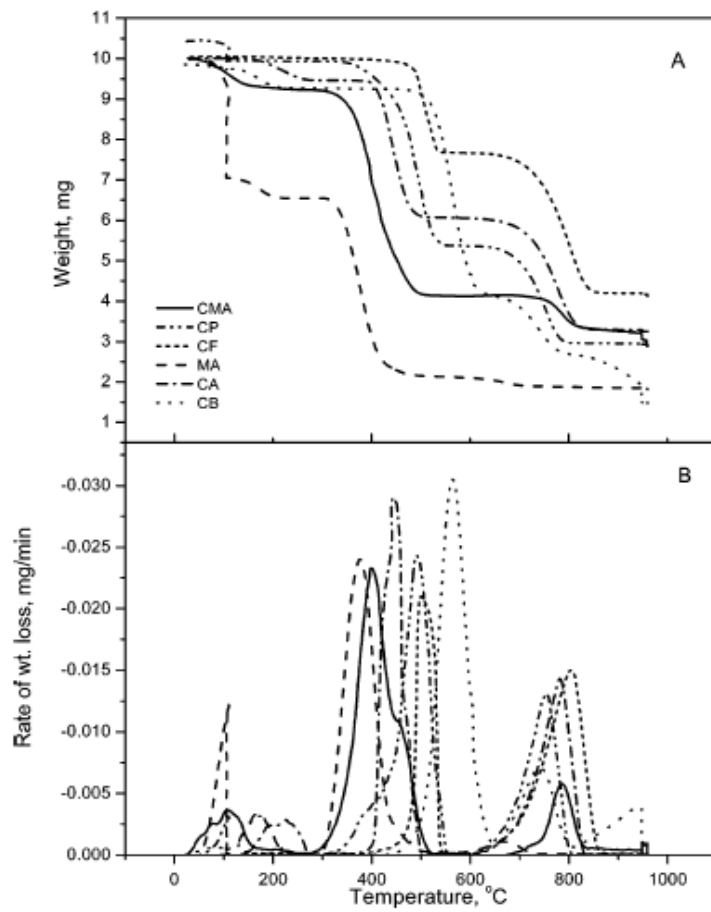


Figure 5. Decomposition profiles from TGA of CMA, CP, CB, CA, MA, and CF. (See figure for legend of line symbols.)

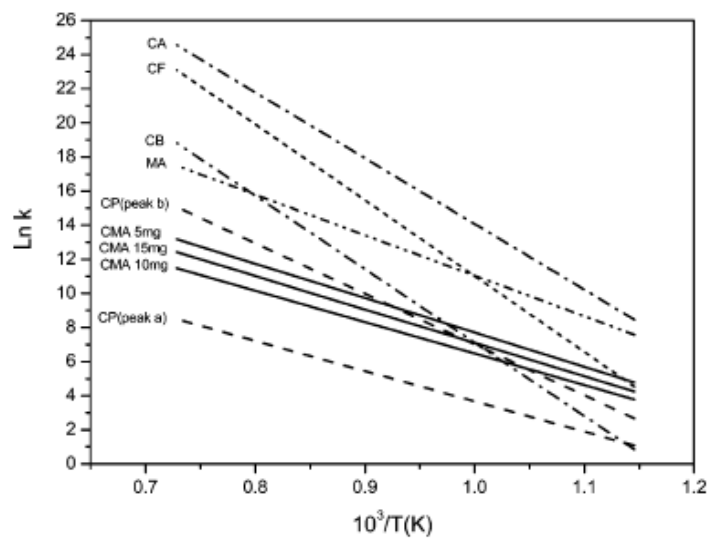


Figure 6. Arrhenius plot of organic decompositions from TG analysis of weight loss data for CMA, CA, MA, CF, CB, and CP.

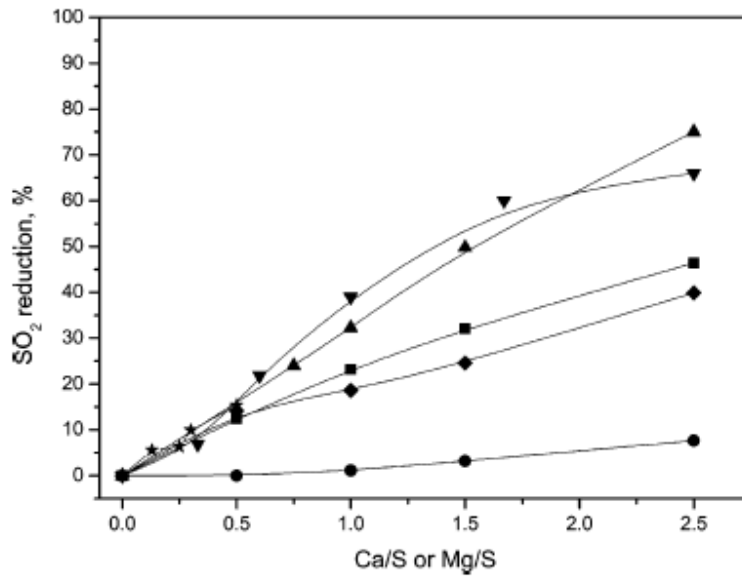


Figure 7. Effect of sorbent feed rate on SO₂ reduction for (▲) CMA, (▼) CP, (★) CB, (◆) CA, (●) MA, and (■) CF, under reburning conditions of $\lambda_1 = 1.05$, $\lambda_2 = 1.03-0.86$, and $\lambda_3 = 1.15$ (3% O₂).

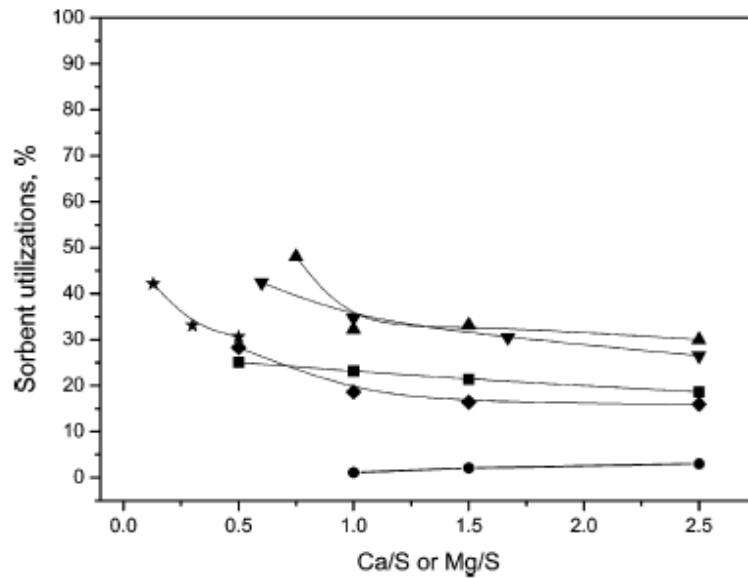


Figure 8. Sorbent Ca and Mg utilizations for SO₂ capture under reburning conditions ($\lambda_1 = 1.05$, $\lambda_2 = 1.03-0.86$, and $\lambda_3 = 1.15$ (3% O₂)): (▲) CMA, (▼) CP, (★) CB, (◆) CA, (●) MA, and (■) CF.

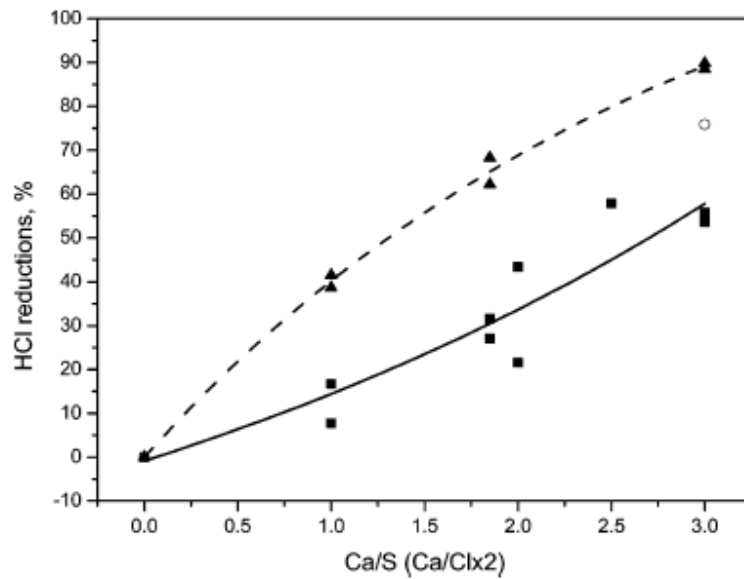


Figure 9. HCl reductions under normal combustion conditions ($\lambda_1 = 1.4$ (6% O₂)) for a range of CMA sorbent feed rates, showing the effect of initial SO₂ concentration (■) 780 ppm, (○) 680 ppm, and (▲) 0 ppm).

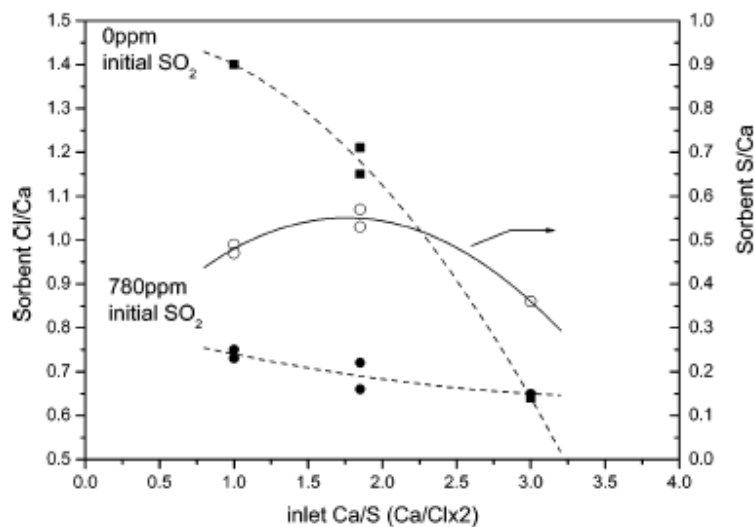


Figure 10. Effect of CMA sorbent feed rate on spent samples; CMA sorbent Cl content for initial SO₂ concentrations of (■) 0 ppm and (●) 780 ppm. Open circles (○) denote the sulfur content.

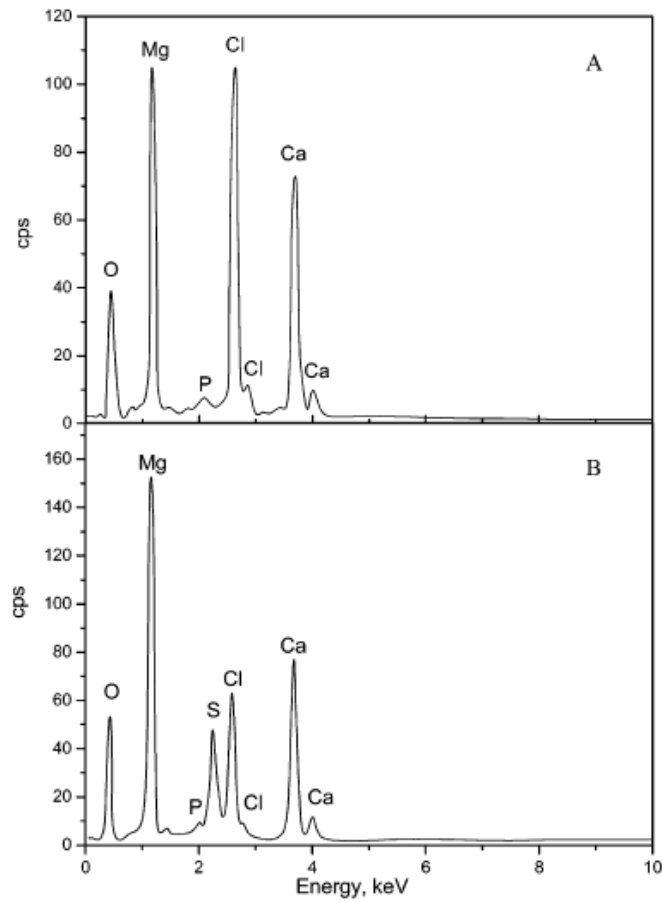


Figure 11. EDX spectrum of samples of spent, CMA sorbent powder for Ca/S = 1.85: (A) sample A, 0 ppm SO₂; and (B) sample B, 780 ppm SO₂.

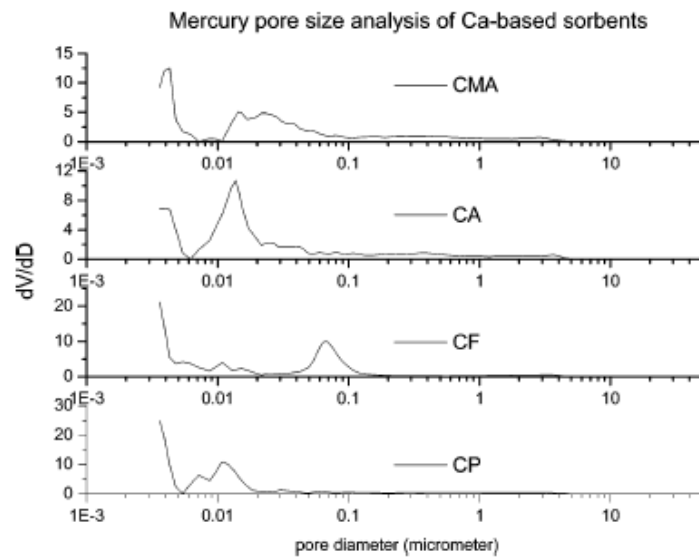


Figure 12. Mercury pore size analysis data for CMA, CP, CA, and CF.

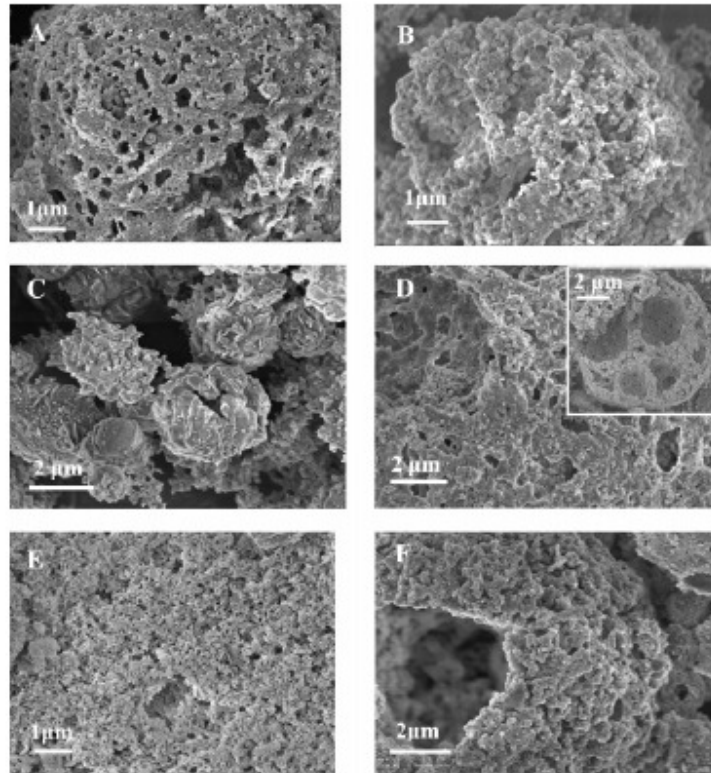


Figure 13. Scanning electron microscopy (SEM) images of reacted sorbent particles after sulfation/reburn: (A) CF, (B) CP, (C) CB, (D) CMA (inset shows a broken particle), (E) MA, and (F) CA.

Table 1. Relationship between Sorbent Feed Rate, as Expressed as Ca/S or Mg/S, to Reburn Zone Stoichiometry (λ_2)^a

λ_2	Sorbent Feed Rate, as Ca/S or Mg/S					
	CB	CMA	CP	CA	MA	CF
0.99 (fuel-lean)	0.53	0.7	1.14	1.77	1.68	4.0
1.0 (stoichiometric)	0.42	0.56	0.91	1.4	1.4	3.15
1.02 (fuel-rich)	0.2	0.35	0.45	0.68	0.89	1.57

^a Legend for table is as follows: CB = calcium benzoate, CMA = calcium magnesium acetate, CP = calcium propionate, CA = calcium acetate, MA = magnesium acetate, and CF = calcium formate.

Table 2. Decomposition Products and Temperatures from Thermogravimetric Analysis (TGA) of Calcium Carboxylic Salts

	Peak 2		Peak 3	
	compound(s)	temp (°C)	compound(s)	temp (°C)
magnesium acetate, MA	2-propanone (acetone), carbon dioxide	376	negligible loss	670
calcium acetate, CA	2-propanone, 2-butanone	444	carbon dioxide, carbon monoxide	779
calcium magnesium acetate, CMA	2-propanone, 2-butanone, carbon dioxide	399/440	carbon monoxide, carbon dioxide	783
calcium propionate, CP	3-pentanone, 3-methyl-2-butanone	390/491	carbon dioxide	754
calcium formate, CF	carbon monoxide, formaldehyde, methanol, carbon dioxide	501	carbon dioxide, carbon monoxide	802
calcium benzoate, CB	carbon dioxide, benzene, benzophenone	557	carbon dioxide, carbon monoxide	745

Table 3. Organics Decomposition Data (Peak 1) from Thermogravimetric Analysis of Carboxylic Salts

salt	initial weight (mg) ^a	activation energy, E_a (kJ/mol)	pre-exponential factor, A (s ⁻¹)	Arrhenius plot correlation coefficient ($n = 1$)
CMA	5	167.3	1.22×10^{12}	0.995
CMA	10	153.4	6.66×10^{10}	0.991
CMA	15	162.9	3.91×10^{11}	0.973
CA	10	321	7.56×10^{22}	0.992
MA	10	197.6	1.31×10^{15}	0.991
CP (1st)	10	147.6	2.01×10^9	0.969
CP (2nd)	10	247	8.7×10^{15}	0.982
CF	10	370.1	1.3×10^{24}	0.989
CB	10	358.2	6.35×10^{21}	0.994

^a With a standard deviation of ± 0.3 mg.

Table 4. Data for the Simultaneous Capture of SO₂ and HCl from Tests in the 80-kW Furnace^a

Ca/S or Ca/Cl $\times 2$	780 ppm initial SO ₂			780 ppm initial SO ₂				0 ppm initial SO ₂		
	SO ₂ (ppm)	SO ₂ reduction (%)	Ca utilization SO ₂ capture (%)	HCl (ppm)	HCl reduction (%)	Ca utilization HCl capture (%)	total (S+Cl) Ca utilization (%)	HCl (ppm)	HCl reduction (%)	Ca utilization HCl capture (%)
0	780	0	0	1500	0	0	0	1500	0	0
1	510	34	34.2	1317	12.2	12.2	46.4	898	40.1	40.1
1.85	330	57	31.0	1024	31.7	17.2	48.2	503	66.5	35.9
2	383	51	25.3	913	39.1	19.6	44.9			
2.5	242	69	27.5	574	61.7	24.7	52.2			
3	230	70	23.4	679	54.7	18.2	41.7	161	89.3	29.8

^a Under normal combustion conditions. $\lambda_1 = 1.4$.

Table 5. Surface Area, Porosity, and Calcination Data of Samples from a Calcination Reactor and an 80-kW_{th} Furnace

	CMA	CA	CF	CP	CMA ^a
BET surface area (m ² /g)	31.8	31.0	23.6	22.7	10.1
N ₂ isosorption					
total pore area (m ² /g)	48.2	47.7	31.4	32.4	
total pore volume (mL/g)	0.24	0.21	0.14	0.16	
average pore diameter (μ m)	0.019	0.018	0.017	0.020	
mercury porosimetry					
total pore area (m ² /g)	50.04	48.19	55.61	55.47	
total pore volume (mL/g)	2.84	2.32	2.15	1.69	
average pore diameter (μ m)	0.23	0.19	0.15	0.12	
porosity (%)	82.6	79.3	73.7	74	
percentage calcination (%)	85.2	80	71.3	84.1	81.8

^a Sample taken from an 80-kW furnace under combustion conditions (propane at 6% O₂).

Table 6. Correlation of NO_x Reduction with Decomposition Kinetics Obtained from the Thermogravimetric Analysis (TGA) of Organic Decompositions for CP, CMA, MA, CA, and CB

	E_{a_s} from TGA (kJ/mol)	NO reduction in the 80-kW furnace (%)	Ca/S or Mg/S	reburn fuel fraction in the 80-kW furnace (%)
CP	148	58	1.25	8
CMA	153	52	2	8
MA	198	55	3	8
CA	321	45	3	8
CB	358	49	0.8	8

Table 7. Particle Size Calculation Data

Estimated Particle Sizes after In-Furnace Spray Calcination		
particle size	typical initial droplet diameter in size range (μ m)	calculated particle size (μ m)
maximum droplet diameter	50	38
minimum droplet diameter	1	0.8
Physical Parameters		
initial droplet concentration		1.6 mol/L
saturation droplet concentration		2 mol/L
density of salt		1.2 g/cm ³
density of oxide		3.3 g/cm ³
oxide yield of salt		0.3
porosity of particle		0.8